

A STUDY OF THE ADHESION AND COHESION OF METALS

By: M. J. Hordon
J. R. Roehrig

Distribution of this report is provided in the interest of information exchange. Responsibility for the contents resides in the author or organization that prepared it.

Prepared under Contract No. NASw-1168
by:

NORTON EXPLORATORY RESEARCH DIVISION
National Research Corporation
Cambridge, Massachusetts 02142

for

NATIONAL AERONAUTICS AND SPACE ADMINISTRATION

FACILITY FORM 602	N66 32677	
	(ACCESSION NUMBER)	(THRU)
	43	1
	(PAGES)	(CODE)
CR-76828		17
(NASA CR OR TMX OR AD NUMBER)		(CATEGORY)

FOREWORD

This interim report summarizes the research effort performed under Contract No. NASw-1168 for the Office of Advanced Research and Technology, National Aeronautics and Space Administration during the period 9 March, 1965 to 9 March, 1966. The program is entitled, "A Study of the Adhesion and Cohesion of Metals" and was administered by Mr. J. Maltz. The research work may be considered as a continuation of the work on metallic adhesion performed under NASA Contract NASw-734.

The project scientists were J. R. Roehrig and Dr. M. J. Hordon. During the initial phase of the program, they were assisted by R. P. Giammanco.

TABLE OF CONTENTS

	PAGE
FOREWORD	iii
ABSTRACT	1
INTRODUCTION	1
APPARATUS	4
General Design	4
Loading Mechanism	4
Wire Brush Abrasion Device	7
Ion Gun Assembly	10
TEST SPECIMEN	13
EXPERIMENTAL PROCEDURE	13
Vacuum Operation	13
Ion Bombardment	16
Adhesion Testing	16
Retarded Field Diode Technique	16
EXPERIMENTAL RESULTS	17
Ion Bombardment Tests	17
Effect of Surface Contour on Adhesion	23
Effect of Mutual Solid Solubility on Adhesion	24
DISCUSSION	32
SUMMARY	34
FUTURE WORK	35

LIST OF FIGURES

FIGURE		PAGE
1	Adhesion Testing Apparatus	5
2	Adhesion Apparatus Loading Mechanism	6
3	Specimen Selector Mechanism	8
4	Wire Brush Abrasion Device	9
5	Ion Beam Gun Assembly	11
6	Installation of Two Ion Beam Guns And Wire Brush Device In Adhesion Test Chamber	12
7	Adhesion Samples	15
8	Ion Energy Distribution for Argon At 2×10^{-7} Torr	18
9	Ion Energy Distribution for Argon At 3×10^{-8} Torr	19
10	Sensitivity Curve For Argon Ion Bombard- ment	20
11	Change In Electron Work Function With Cleaning Time At 2×10^{-7} Torr With Argon Ion Bombardment	22
12	Variation Of The Adhesion Coefficient With Yield Coefficient For Soluble and Insoluble Metal Pairs	27
13	Adhesion Coefficient Dependence On The Yield Strength	30
14	Temperature Dependence Of The Adhesion Coefficient	31

A STUDY OF THE ADHESION AND COHESION OF METALS

By M. J. Hordon

J. R. Roehrig

National Research Corporation

SUMMARY

32677

Measurements of the adhesion characteristics of a variety of metals were conducted in high vacuum. The contact surfaces were cleaned prior to loading by argon or xenon ion bombardment or by wire brush abrasion. The applied loads exceeded the nominal yield stress. Although the ion bombardment produced substantial changes in the surface electron work function as determined by the retarded field diode technique, the resultant adhesion values were generally negligible. Smooth, flat surfaces of copper showed greater bonding than roughened surfaces.

Using the abrasion method, the adhesion of both soluble and insoluble metal pairs was studied. The results showed that lattice solid solubility was less important than surface cleanliness and ductility in governing the extent of interfacial welding. Under optimum conditions, bond efficiencies up to 90% were obtained for extremely ductile metals.

INTRODUCTION

Research on adhesion and bonding phenomena at vacuum levels from 10^{-6} to 10^{-13} torr and at temperatures ranging from 20° to 200°C has been carried on at National Research Corporation for the last several years under NASA Contracts NASr-48, NASw-734 and NASl-2691 and Air Force Contract AF 04 (611)-9717. The general objective has been to obtain detailed information on the conditions governing the tendency of engineering metals and alloys to adhere to one another under contact loading. Sufficient bonding force was frequently observed to prevent or hinder the relative motion or subsequent separation of component surfaces even after exposure for as much as one minute at 10^{-7} torr after cleaning the mating surfaces in ultra-high vacuum.

Information of this nature is of obvious interest in the design of electrical and mechanical devices for space vehicle application. Typical spacecraft devices with critical bearing or contacting surfaces include solenoids, valving, slip rings, bearings and various types of mating flanges, sockets and pins, etc. In addition, the adhesion behavior of various materials has a primary application in cold welding processes in which large scale bonding is sought while minimizing excessive temperature and plastic deformation levels. It may be noted that solid adhesion is of basic interest in studies of the physics of surfaces, a field of expanding importance in materials science.

The experimental results of adhesion studies carried out at National Research Corporation may be summarized as follows:

1. Adhesion bonding requires the removal and continued absence of organic and oxide adsorbed films.
2. Adhesion is increased with increased compressive loading, particularly for loads high enough to cause plastic yielding at the interface.
3. Adhesion is increased with increasing temperature and longer times at temperature.
4. Partial bonding has been observed with proper surface treatments between metals with limited mutual solid solubility.
5. With pre-cleaning of surfaces by methods such as wire brushing in vacuum, bonding force to compressive load ratios up to 60 percent have been attained at room temperature for ductile metals provided the contact stress exceeded the yield stress.

It is apparent from these results that substantial adhesion may be expected between mating surfaces in the low pressure environment of space provided sufficient deformation or abrasion occurs to break up the existing oxide layers originally formed in the earth's atmosphere.

In the present work, several of the parameters controlling the extent of macroscopic bonding were selected for detailed examination. Of major importance in forming a strong bond across the interface is the relative amount of metallic surface area brought into close atomic contact. Two factors which critically affect the degree of metal-to-metal contact are the formation of oxide or contaminant surface films with rigid crystal structures of low coordination number and the surface micro-topography or contour. It is evident that an intervening oxide layer or large deviations from atomic planarity can severely limit the actual metallic contact over the nominal bearing area.

The effect of surface cleanliness and contour on metallic adhesion was studied in the current investigation using xenon ion bombardment as a surface cleaning technique in order to minimize damage to the contact area. The degree of contaminant film removal as a function of ion bombardment dosage may be estimated by monitoring changes in the relative surface electron work function as determined by retarded field diode measurements.

One parameter of interest in adhesion phenomena is the effect of mutual solid solubility in solid state bonding. It had been postulated that even under conditions in which good metallic contact was made, large scale adhesion would not occur unless the contact materials formed extensive solid solutions in each other. For metals that are insoluble in each other, e.g., form A-A and B-B bonds in preference to A-B bonds within the lattice, it was held that the unfavorable energy barrier would substantially prevent A-B bonding across the interface. It was decided to test this hypothesis by comparing the adhesion characteristics of both soluble and insoluble metal pairs with similar mechanical properties under equivalent conditions.

The general object of this investigation was to examine the effect of selected material on the bonding strength in order to provide a clearer picture of the physical mechanisms underlying solid state adhesion at temperatures below the range in which diffusion bonding becomes the controlling process.

APPARATUS

General Design

The adhesion testing apparatus used in the present work is a modified design incorporating the basic features of the apparatus used for adhesion testing on NASA Contract No. NASw-734. As shown in Fig. 1, it consists of a cylindrical, stainless steel ultra-high vacuum chamber 14 in. in diameter. The chamber contains several viewing ports, two ports for the introduction of the ion beam guns, one port for the use of a mechanical wire abrasion device, two ports for manipulative mechanisms and a pressure sensing gauge port.

The loading assembly, illustrated in Fig. 2, is an integral part of the upper flange head. The loading shaft contains a ball and screw drive mechanism which can impose loads up to 2200 lbs on the lower anvil. The linear thrust of the shaft is introduced into the vacuum chamber via a flexible bellows seal. A rigid compression cage fixture is provided to guide the motion of the shaft and insure vertical alignment of the loading stages. Loading may be performed either by a motor driven chain drive or by manual operation of a rotary drive. The resultant force is monitored by a load cell with electronic read-out.

The vacuum chamber is evacuated by a standard NRC 10 in. diffusion pump through a right angled refrigerated trap and two internal liquid nitrogen traps. The system also contains an NRC 2 in. diffusion pump and a mechanical pump for preliminary evacuation. Concentric "o"-ring seals at the flanges are refrigerated or water cooled to eliminate outgassing. The exit port to the pump is also refrigerated with cooling coils. Thermal outgassing of the vacuum chamber up to 250°C can be maintained by internally mounted quartz rod heaters. The vacuum system when fully loaded with the adhesion testing components is capable of pressures down to 8×10^{-10} torr after outgassing.

Loading Mechanism

Integral parts of the loading mechanism are the multi-station specimen loading stages which can sequentially select up to eight adhesion pairs for testing in one pumping operation.

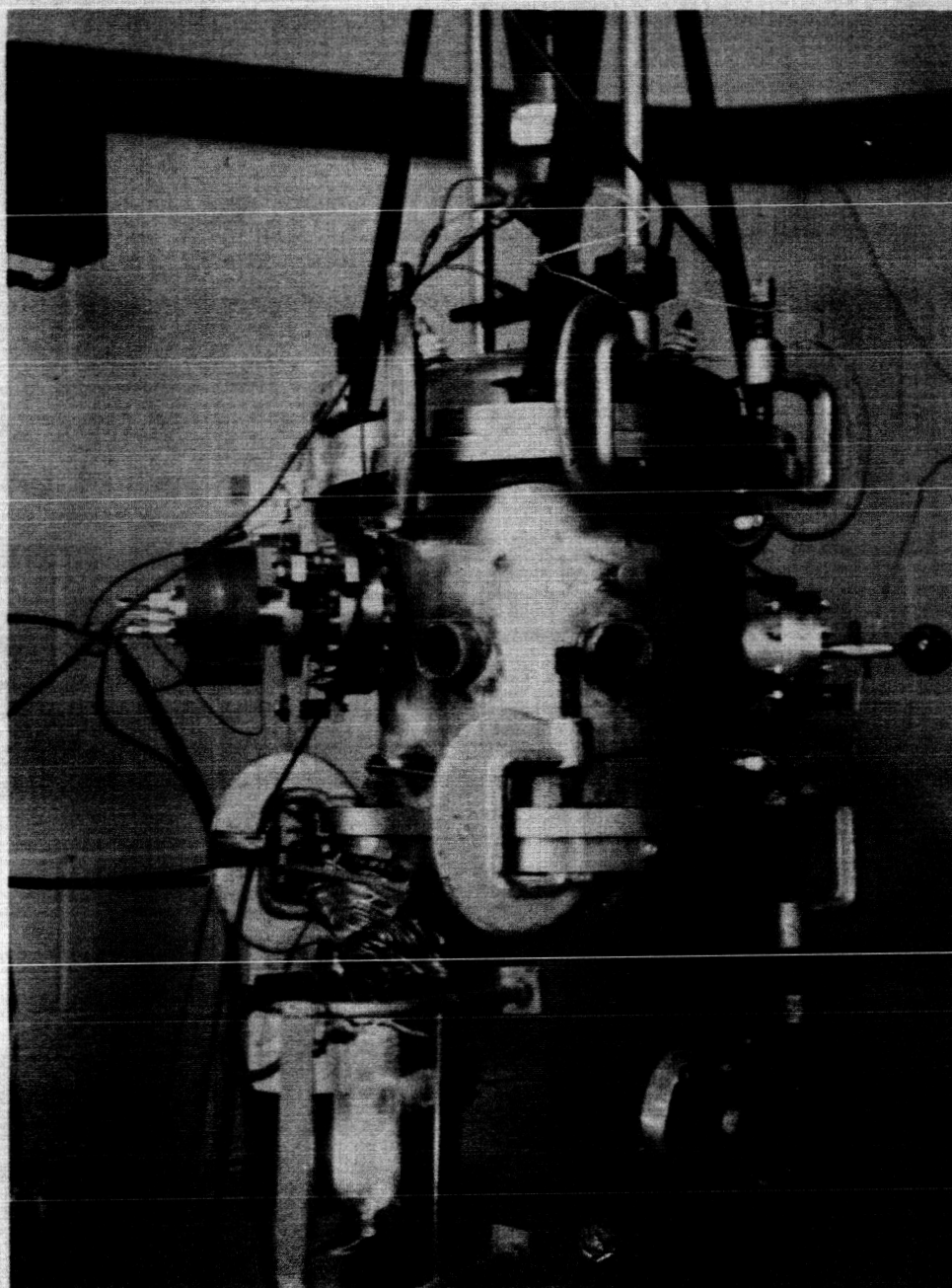


Fig. 1

ADHESION TESTING APPARATUS

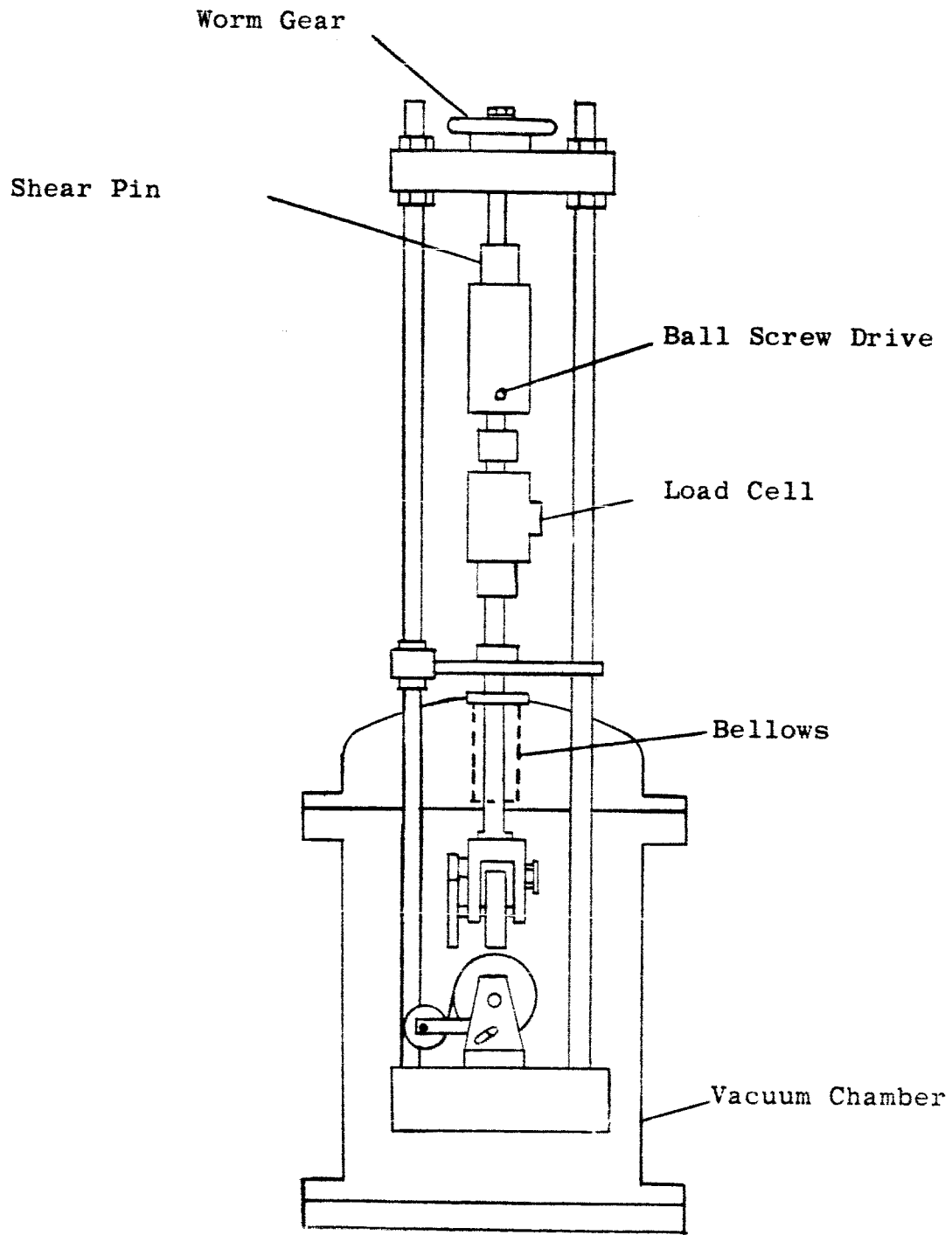


Fig. 2 ADHESION APPARATUS LOADING
MECHANISM

These components consist of two rotating stainless steel wheels mounted on the loading shaft and the lower anvil. Specimen samples are mounted in eight recesses provided on the wheel rims.

Due to the requirement that the specimens selected for test be brought to a horizontal position in the ion bombardment technique and then to a vertical position for loading, rapid rotation through 90° is necessary to minimize the possibility of oxide film re-formation after bombardment.

To reduce the time required for rotation, the loading stages were modified by the addition of a weight-actuated pulley mechanism illustrated in Fig. 3. In this arrangement, operation of a double pin device by manual manipulation through a flexible bellows seal permitted rapid rotation of any station through 90° . The positioning change for both stages required less than 6 sec. between bombardment and loading sequences. The pulley mechanism was selected in place of a spring-actuated mechanism because of the necessity to heat the chamber to 250°C for outgassing. Attempts to use a negative-torque spring drive for rapid specimen selection showed that the springs were annealed beyond their useful range at this temperature level.

Wire Brush Abrasion Device

The vacuum assembly also contains a wire brush abrasion device for scouring contaminant films from the test surfaces immediately prior to contact. The cylindrical brush is mounted on a flexible bellows seal to permit manual manipulation from outside the chamber. Rotary power is provided by a compact vacuum sealed motor integrally mounted on the brush shaft. In practice, the stainless steel brush is brought to bear on the two test surfaces simultaneously as shown in Fig. 4. After an abrading for 2 to 5 min., the brush is removed and the test surfaces are brought into contact. The elapsed time between brushing and contact is about 8 - 10 sec.

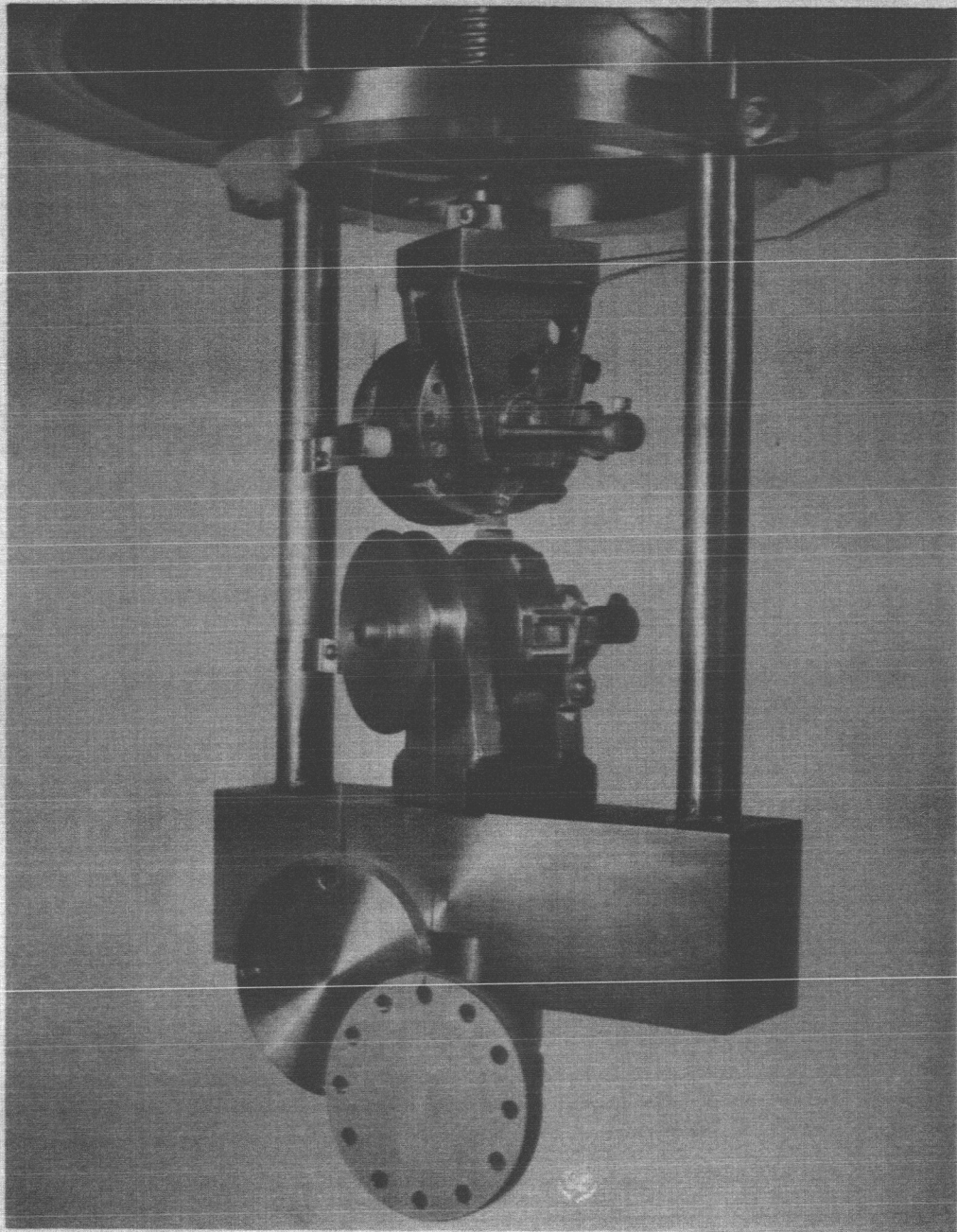


Fig. 3

SPECIMEN SELECTOR MECHANISM

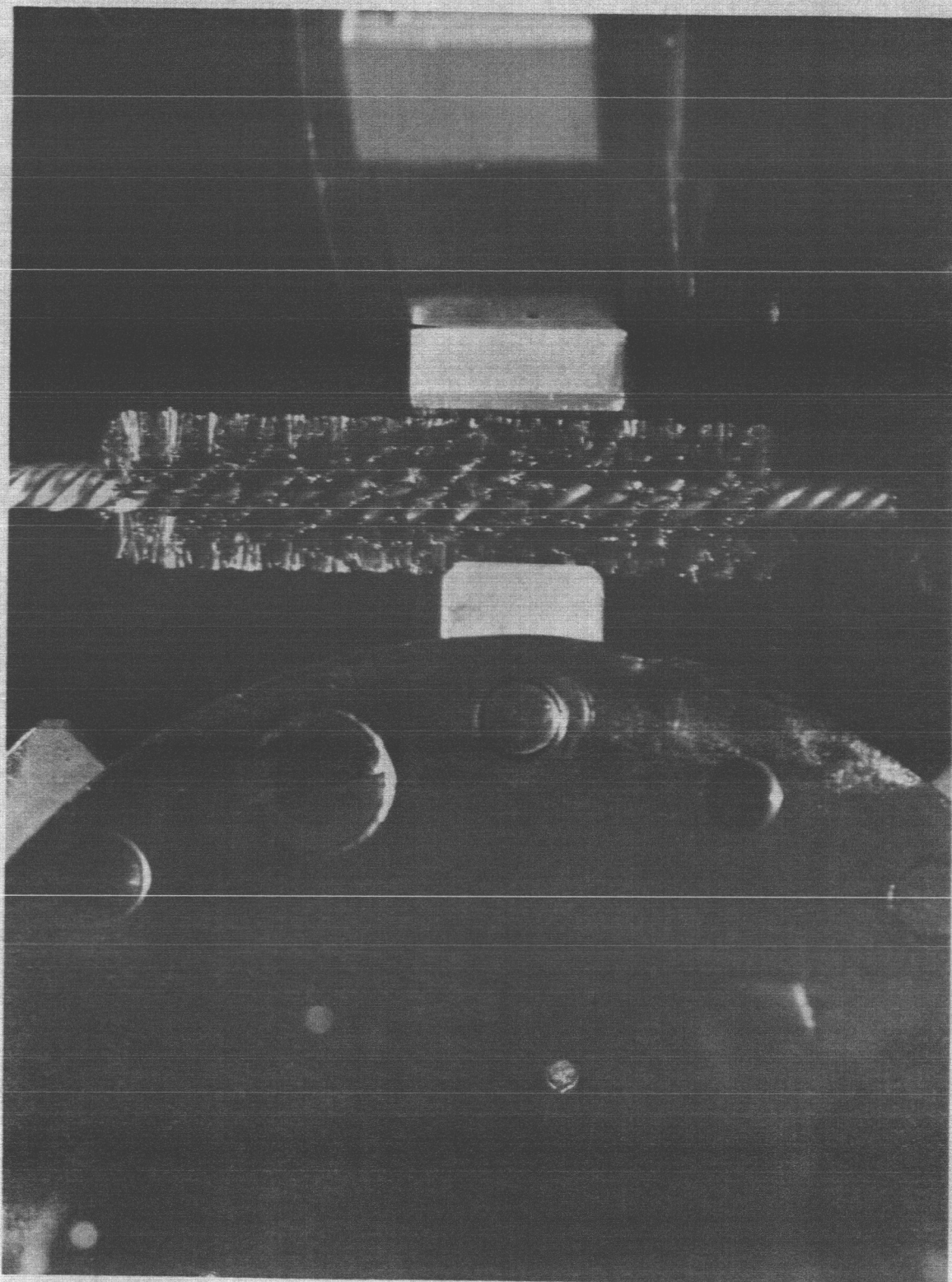


Fig. 4
WIRE BRUSH ABRASION DEVICE

Ion Gun Assembly

Since the brush abrasion technique necessarily roughens the surface severely, it was considered desirable to devise an inert gas ion beam cleaning method for both contact surfaces in examining the effect of surface profile on adhesion strength. Because the mating surfaces cannot be brought close together in the test apparatus except in the parallel position, two separate ion gun assemblies were required to bombard each surface independently. In order to accomplish this in the limited space available in the vacuum chamber, it was planned to mount the two guns on the side of the cylindrical chamber at positions 90° apart. In this way, the ion beams could be focused independently on the specimen surfaces when rotated to the horizontal position on the loading mechanism.

An individual gun assembly is shown in Fig. 5. Consisting essentially of a cold cathode ion source based on the Red-head cold cathode magnetron gage which can ionize a partial pressure of xenon or argon gas bled into the central cavity, the gun can direct an energized stream of ions to the target surface by means of a series of einzel lenses. The magnet components are mounted outside the gun cavity to permit removal during thermal outgassing. The ion stream is directed into the vacuum chamber through a narrow orifice to minimize pressure build-up in the main chamber.

In practice, anode voltages up to 6000 volts at 1×10^{-6} amp can be consistently obtained, yielding ion current densities up to 12 amp/torr - cm^2 at the target surface. In the usual operating condition, the partial pressure of inert gas in the gun cavity may be 10^{-2} torr; the corresponding system pressure will rise to $2 - 5 \times 10^{-7}$ torr during bombardment. In use, the ion stream may be deflected by manual operation of a bellows seal spring assembly thus permitting accurate focusing of the beam on the target. Focusing is accomplished by monitoring the optimum current peak during the deflection adjustment.

The installation of the gun assemblies in the vacuum chamber is shown in Fig. 6. The radial magnet components are shown in position. Each gun assembly is provided with a Granville-Phillips bleeder valve which admits a controlled quantity of high purity xenon gas to the gun cavity through a 0.040 in. inlet tube. The deflection spring coils providing angular movement of the gun axis at the flexible bellows seal are also shown.

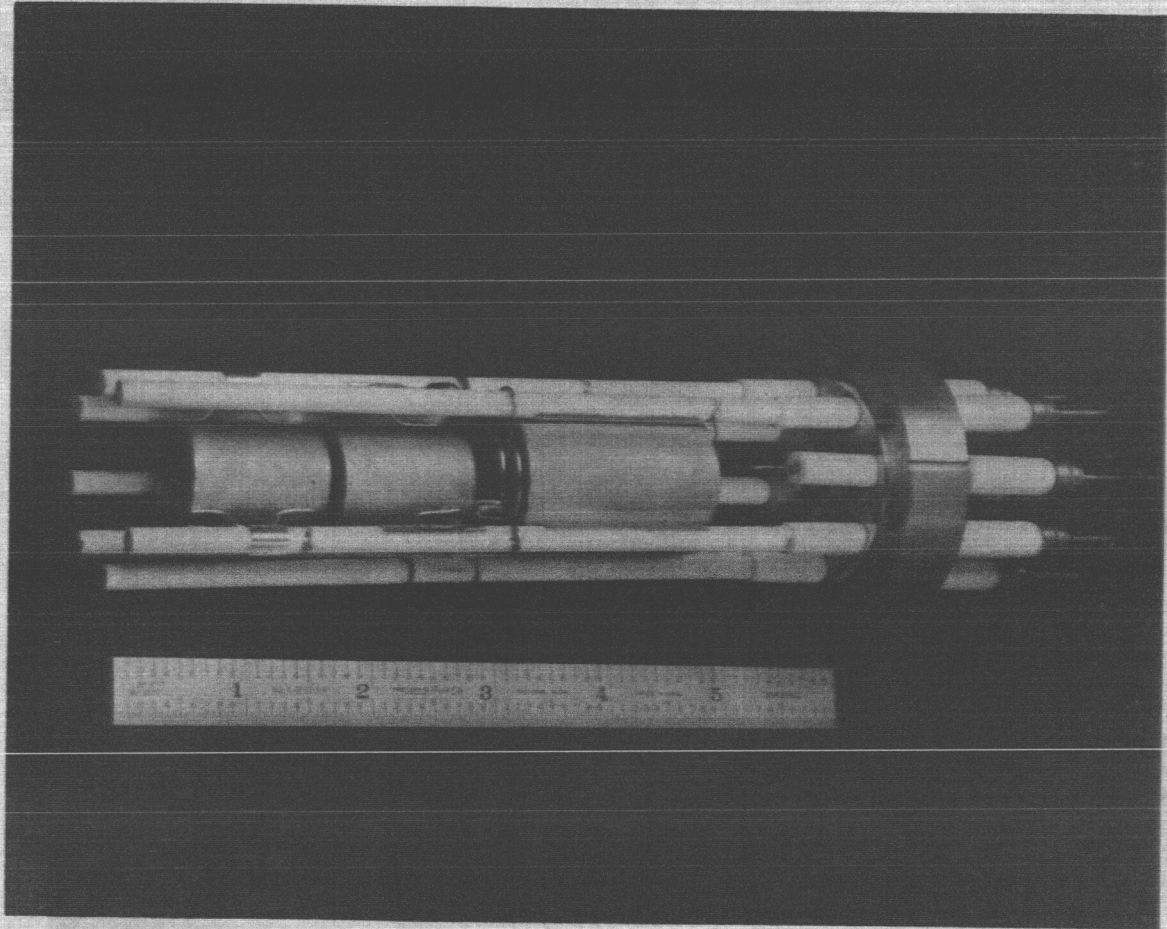


Fig. 5

ION BEAM GUN ASSEMBLY

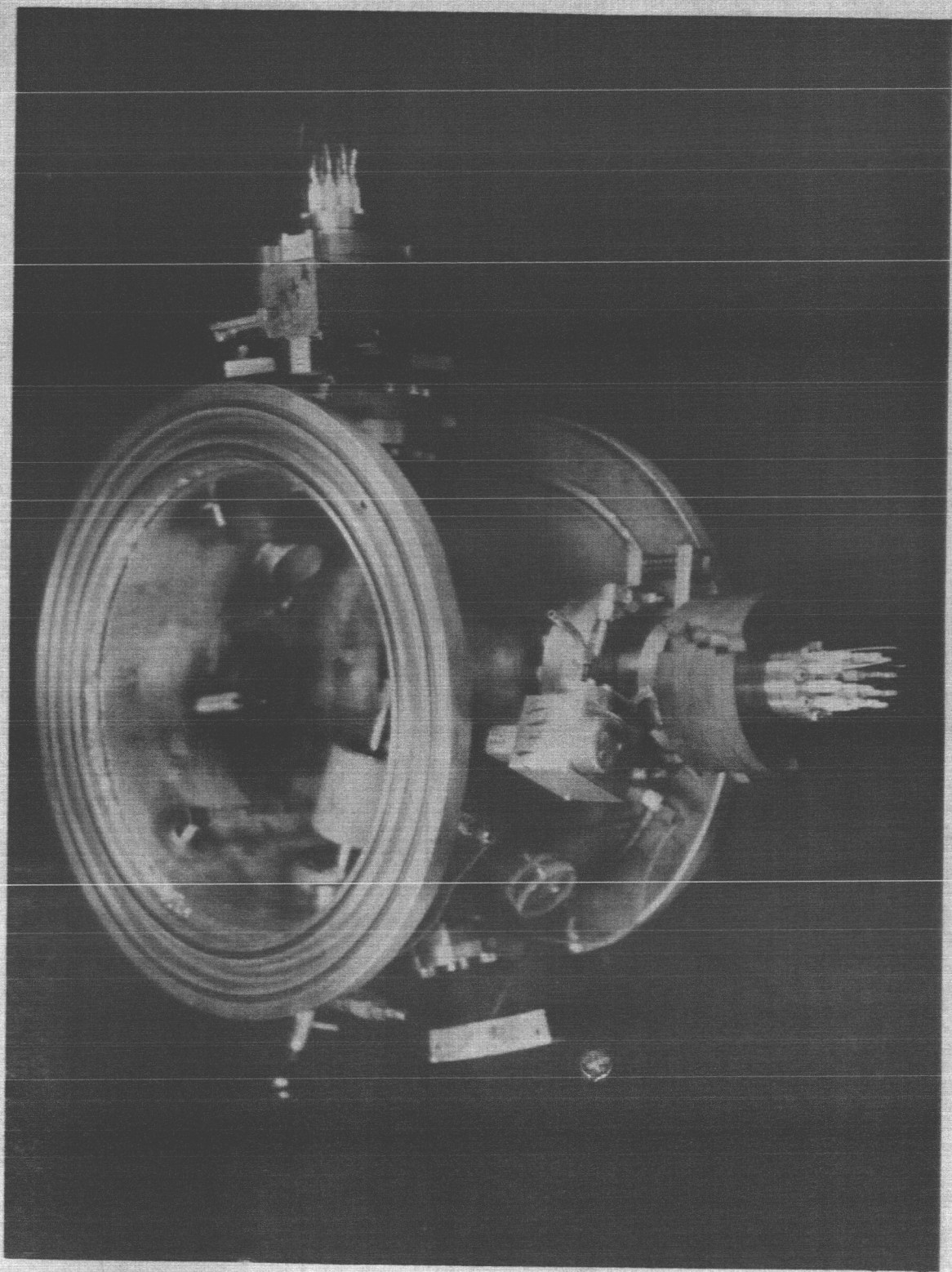


Fig. 6
INSTALLATION OF TWO ION GUNS AND WIRE BRUSH DEVICE IN ADHESION TEST CHAMBER

TEST SPECIMENS

Adhesion samples were prepared of various pure metals as listed in Table I. The sample configuration is illustrated in Fig. 7. Since the upper and lower samples are crossed at right angles to each other in the loading stages, for the maximum load of 2200 lbs, the corresponding nominal bearing stress was about 15,700 psi.

In order to obtain higher contact stresses for high strength materials, it was necessary to decrease the bearing area by beveling the edges of the sample as shown in Fig 7b. In this way, the nominal contact stress could be adjusted to a level exceeding the compressive yield strength of the samples. For the metals used in this work, the bearing area of iron, niobium, tantalum and nickel samples was decreased to permit higher stresses.

Samples were fully annealed after machining and tested for hardness prior to use. The mechanical properties of the metals are listed in Table I. In the case of gold, the sample geometry was modified by brazing annealed gold strip 0.040 in. in thickness to a copper block. The composite sample had the same final dimensions as other specimens. After machining, the sample contact surfaces were metallographically polished and checked for flatness.

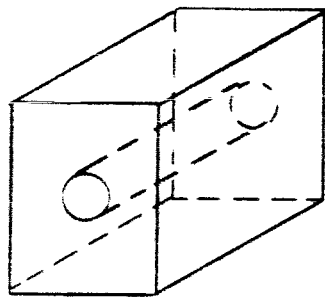
EXPERIMENTAL PROCEDURE

Vacuum Operation

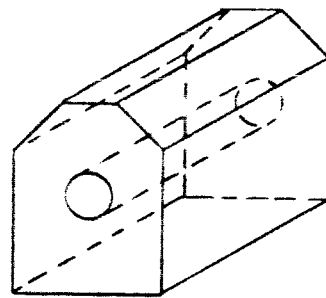
For adhesion tests which utilized wire brush abrasion for sample cleaning, the selected samples were rotated to the vertical position facing each other and separated by a 0.5 in. gap. The stainless steel brush was then brought to abrade both surfaces simultaneously for periods exceeding 2 min. During the abrasion operation, gas evolution from the surfaces was observed which yielded pressure transients up to 2×10^{-8} torr depending on the metal sample.

TABLE I
Sample Composition and Properties

Metal	Purity (%)	Heat Treatment	Hardness (BHN)	Yield Strength (psi)
Copper	99.† (OFHC)	500°C, 0.5 hr.	45	9,000
Silver	99.9	as-received	40	7,900
Nickel	99.†	1050°C, 0.5 hr.	110	15,000
Gold	99.9†	as-received	25	2,000
Lead	99.9†	as-received	15	1,200
Iron	99.8†	700°C, 0.5 hr.	75	18,000
Tantalum	99.9†	1050°C, 0.5 hr.	79	39,000
Niobium	99.7†	1050°C, 0.15 hr.	35	32,000



(a)



(b)

Fig. 7 ADHESION SAMPLES

At the end of the cleaning period, the brush was removed and the samples brought into contact. With the motor driven chain drive, the elapsed time between brushing the contact was 14-20 sec. However, manual operation of a rotary screw drive lowered the elapsed time to about 10 sec. At an average system pressure about 4×10^{-9} torr, the exposure product, about 1×10^{-9} torr-min, is below the oxide formation time required for 1/10th monolayer coverage. Hence, bare metal contact was achieved.

Ion Bombardment

For adhesion tests utilizing gas ion bombardment for sample cleaning, the selected samples were rotated to horizontal positions facing the ion guns. At pressure levels below 1×10^{-9} torr, the guns were activated by bleeding into the system a partial pressure of xenon or argon purified gas. During bombardment, the pressure rose to about $2 - 5 \times 10^0$ torr.

In operation, the ion guns were focussed by deflection lenses onto targets positioned adjacent to the adhesion samples. Operating voltages in the range 3,000 - 6,000 volts at $3 - 5 \times 10^{-7}$ amp were maintained for periods up to 5 hrs. The ion guns were independently controlled and focussed.

At the end of the cleaning period, the specimens were rapidly brought into the vertical position and into contact using the pulley mechanism for fast rotation. Elapsed time periods between cleaning and contact of about 6 sec. were routinely attained.

Adhesion Testing

Upon contact, the sample pair were brought to the desired load and held constant for a five min. period. The separation force if any, was measured optically by a load-strain recorder with a sensitivity of ± 10 lbs. In some cases, the specimen pairs were retained in the welded condition. Upon removal from the vacuum system, the sample pairs were examined metallographically.

Retarded Field Diode Technique

In research programs concurrent with the present work, a technique was developed to estimate the degree of surface cleaning produced by ion bombardment by monitoring the relative

change in electron work function values. The work function of the bombarded surface can be determined by the extrapolation of the limiting values of retarded potential curves. Such plots are derived from measurements of the electron current as a function of the accelerating potential between the specimen surface and a standard tungsten emitter acting as a diode.

In this technique, the diode assembly is positioned in the vacuum chamber so that the target surface becomes one half of the diode. Upon interrupting ion bombardment after various dosages, the voltage-current characteristics of the diode are recorded. The slope of the current-voltage plot in the negative potential range is then linearly extrapolated to the value of the current corresponding to the saturation limit at maximum positive potential. The work function can then be defined as the voltage gap between the extrapolated negative potential and zero potential.

EXPERIMENTAL RESULTS

Ion Bombardment Tests

Measurements of ion gun performance and the necessary calibration tests were conducted on both gun units designed for specimen surface cleaning. Using purified argon gas, ion energy distribution curves were plotted for various voltage configurations. Representative ion energy distribution curves for a focused beam are given in Figs. 8 and 9 for anode potentials up to 8000 volts.

Based on these curves it is evident that the ion impingement energy is highly dependent on the anode voltage. Typically, the maximum ion kinetic energy is about 1/5 the anode potential. By carefully adjusting the permanent magnet beam deflectors controlling the ion dispersion, it is possible to increase the efficiency of the gun to somewhat higher levels.

A representative calibration curve for argon gas is shown in Fig. 10 as a function of the anode potential. The current density represents the ion current flux arriving at the target surface at the indicated gas partial pressures.

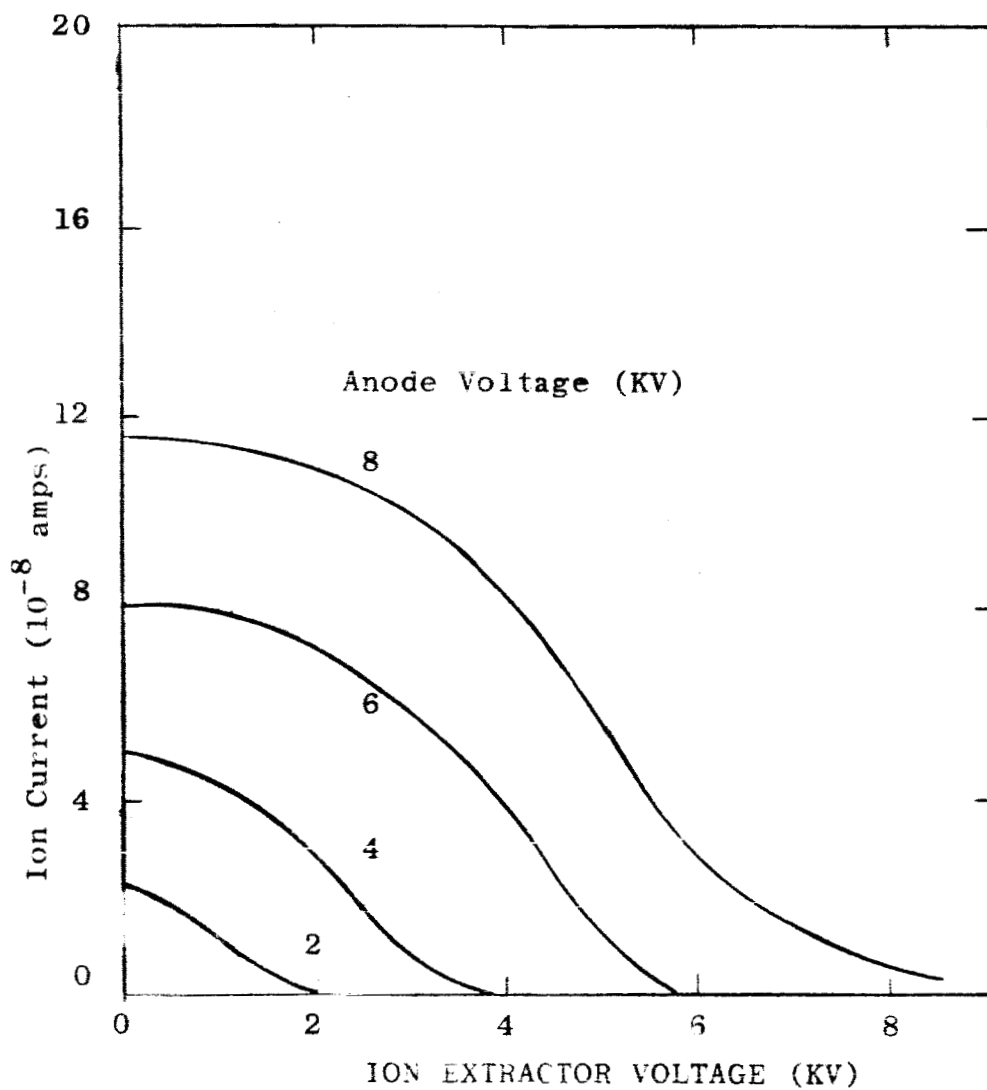


FIG. 8

ION ENERGY DISTRIBUTION FOR ARGON AT
 2×10^{-7} TORR

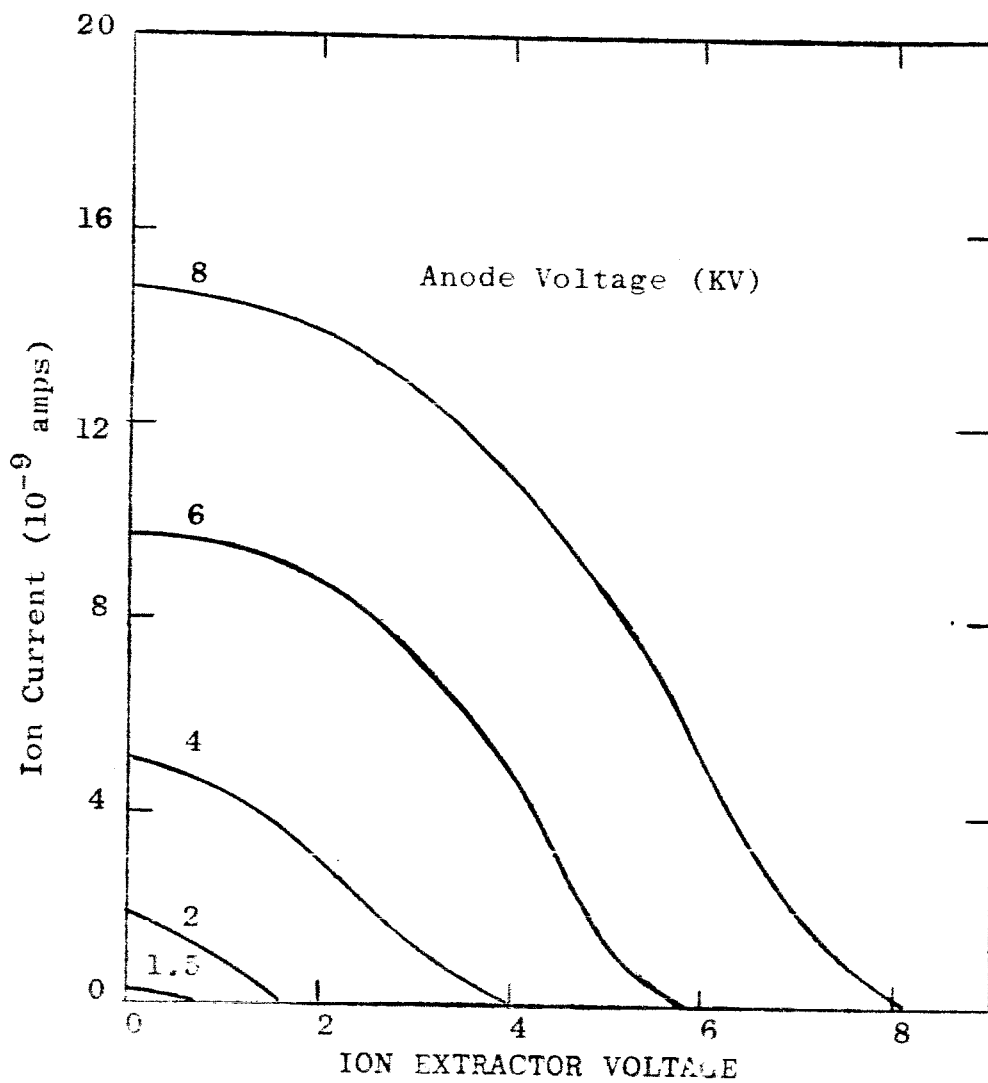


FIG. 9

ION ENERGY DISTRIBUTION FOR
 ARGON AT 3×10^{-8} TORR

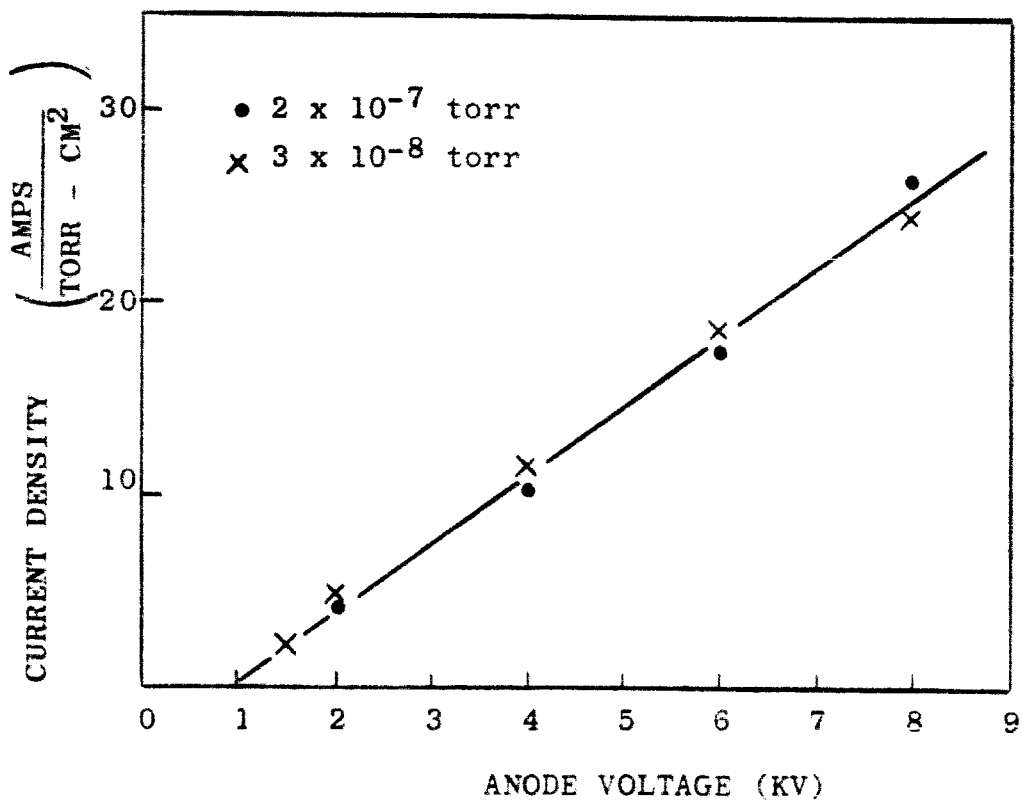


Fig. 10 Sensitivity Curve For Argon Ion Bombardment.

It is evident that the current density was relatively insensitive to the argon gas pressure below 10^{-7} torr. The total ion dosage may then be taken as the ion current density multiplied by the bombardment time. In operation, the usual bombardment dosages were in the range 10-70 amp-hr/torr - cm^2 .

The effectiveness of ion bombardment in removing existing surface atoms was evaluated for tungsten metal using the retarded field diode technique to monitor the electron work function of the irradiated surface. The retarded potential curve is a plot of the variation of electron beam current with applied potential into the negative voltage region. As the diode potential is decreased below zero volts, the diode current is rapidly decreased to negligible values. The slope of the current decay in the negative voltage range may be taken as a function of the surface electron work function or energy barrier for removing electrons from the metal surface.

Using a tungsten target and tungsten wire ribbon as the diode, a relative change in the electron work function $\Delta \phi = -0.6$ volts was obtained after prolonged argon ion bombardment compared with the original surface. The effect of bombardment dosage on the change in work function of irradiated copper and tungsten samples is shown in Fig. 11. A constant ion impingement rate of approximately 10^{10} ions/ cm^2 was maintained. At selected time intervals, bombardment was interrupted and the relative change in surface work function evaluated. It is apparent that the bombardment produced well defined changes in work function indicating the probable removal of surface atom layers on the target.

It may be noted that after 10 hours of bombardment, the samples were permitted to recontaminate for periods up to 24 hrs. at an average pressure of 2×10^{-9} torr. Generally, the original work function value was not regained. It may be postulated that this behavior was due to the extremely low partial pressure of oxygen in the system which effectively retarded the reformation of extension oxide films.

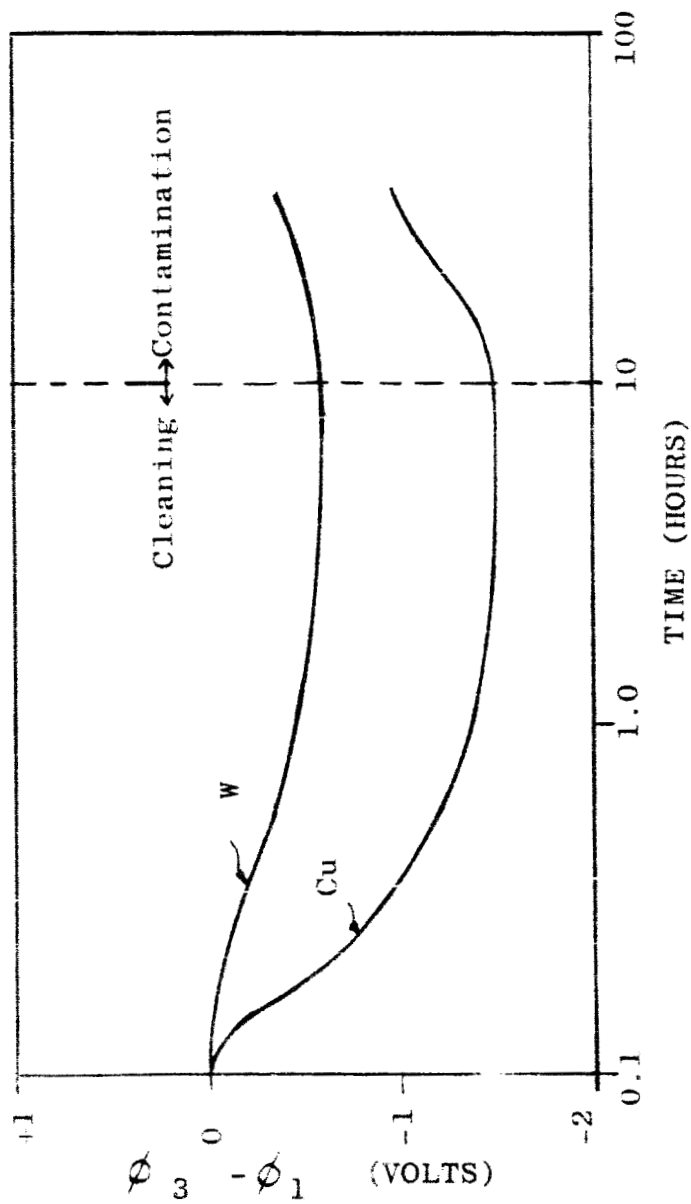


Fig. 11 Change in Electron Work Function With Cleaning Time At 2×10^{-7} Torr With Argon Ion Bombardment

A series of adhesion tests utilizing samples of polished copper and silver were conducted using xenon ion bombardment as the surface cleaning technique. Bombardment dosages up to 50 amp-hr/torr-cm² were used for both ion guns independently irradiating the two contact surfaces. Initial pressure levels of about 7×10^{-10} torr before bombardment rose to about 5×10^{-6} torr as xenon gas was bled into the chamber to operate the guns. After bombardment in the horizontal position, the samples were rotated to the vertical position and loaded to 2000 lbs. The nominal contact stress was about 30,000 psi.

Preliminary results showed that negligible adhesion was obtained after ion bombardment for both copper and silver samples. Analysis of the test data showed that an important parameter was the elapsed time between the end of bombardment and full contact. In the early tests, this time frequently exceeded 60 sec. due to difficulties in accurately positioning the samples in the loading procedure. At an average vacuum level of about 5×10^{-9} torr, this exposure time probably allowed some reformation of the oxide film and prevented extensive bare metal contact.

With the improved pulley-actuated rotation mechanism installed, the elapsed time was reduced to about 6 sec. A second series of adhesion tests using the improved mechanism was conducted with copper and silver samples. In this series of tests, slight self-adhesion of copper was noticed; the separation force was about 10 lbs. close to the limit of detection. The self-adhesion of silver was negligible. It may be noted that the bonding strength in copper after ion bombardment was considerably less than the bonding forces observed after abrasive cleaning. In previous tests with wire brush abrasion, the bonding force for copper frequently exceeded 400 lbs. for a compressive loading of about 1200 lbs.

Effect of Surface Contour on Adhesion

Measurements of the self-adhesion of copper and silver samples were made as a function of contact surface finish in order to determine the effect of surface profile on the bonding characteristics. Sample pairs of both metals

were prepared with metallographically polished surfaces with a height variation less than 4 microinches rms. Sample pairs were also produced with roughened surfaces by vapor blasting with local height variations exceeding 60 microinches rms.

The smooth and rough contact surfaces were cleaned by intensive argon gas bombardment for periods up to 5 hrs at the maximum current density capacity of the ion guns. Exposure times between bombardment and load contact were below 10 sec. at an average system pressure of 1×10^{-9} torr. The contact stress was about 30,000 psi.

The results for copper showed slight residual bonding for polished samples frequently approaching 10-15 lbs force to effect separation. On the other hand, the roughened surfaces showed negligible bonding. Both sets of silver samples again showed negligible adhesion. The composite results are listed in Table II.

It was apparent that the ion bombardment procedure presently employed was not effectively stripping the silver oxide layers from the sample surfaces, although partial cleaning was occurring for the copper samples.

Effect of Mutual Solid Solubility on Adhesion

In order to determine the effect of solid solubility on surface bonding, eight pairs of unlike metals were prepared for adhesion testing. Four of the pairs were composed of metals exhibiting complete solubility in each other at all temperatures, the remaining four combinations comprised metals showing negligible mutual solid solubility at room temperatures. The following metal pairs were tested:

Soluble Pairs

Cu-Au
Cu-Ni
Ag-Au
Nb-Ta

Insoluble Pairs

Cu-Ta
Ag-Fe
Ag-Ni
Au-Pb

TABLE II

Adhesion Characteristics of Ion Bombarded Metals

Maximum Separation Force (lbs)⁽¹⁾

	<u>Copper</u>	<u>Silver</u>
Polished Surface (< 4 μ rms)	10-15	0
Roughened Surface (> 60 μ rms)	0	0

(1) Standard compressive load of 2000 lbs (~30,000 psi).

Upon positioning the samples in the correct sequence in the loading stages, standard evacuation procedures were used to obtain an average vacuum level of about 5×10^{-9} torr. The specimens selected for test were rotated to the vertical position and abraded with a stainless steel wire brush for periods of about 2 min. During the cleaning period, pressure bursts up to 2×10^{-8} torr were observed. After abrasion, the samples were brought into loaded contact with an elapsed time of about 16 sec.

In order to compare the results on an equivalent basis, the compressive load for each pair was adjusted to take into account the magnitude of the yield stress of the softer metal. Previous investigations have shown that extensive bonding would only occur, provided the contacting surfaces were clean, when the contact stress exceeded the yield stress. In the present work, the ratio of the applied normal stress S_N to the lowest yield stress S_Y , defined as the yield coefficient, was maintained in the range 1.0 to 2.0. Comparison of the adhesion behavior of soluble and insoluble metal pairs were made for equivalent S_N/S_Y ratios.

The results of the adhesion testing for both sets of samples at room temperature are shown in Fig. 12 in which the adhesion coefficient, defined as the ratio of the maximum separation or rupture stress S_r required to break the welded samples to the applied normal compressive stress S_N , is plotted against the yield coefficient S_N/S_Y . It is evident that the adhesion coefficient generally increased with the yield coefficient indicating the importance of ductility in enhancing bare metal contact.

It is extremely interesting to note that insoluble metal pairs as well as soluble pairs showed well defined bonding characteristics. Indeed, the highest adhesion coefficient (~ 0.6) was obtained for the insoluble lead-gold couple whereas the lowest bonding strength was obtained for the niobium-tantalum pair (~ 0.1). These results appear to indicate that metal ductility and interfacial contact have a substantially more important effect in controlling large scale adhesion than the intrinsic strength of the unit atomic bond across the interface.

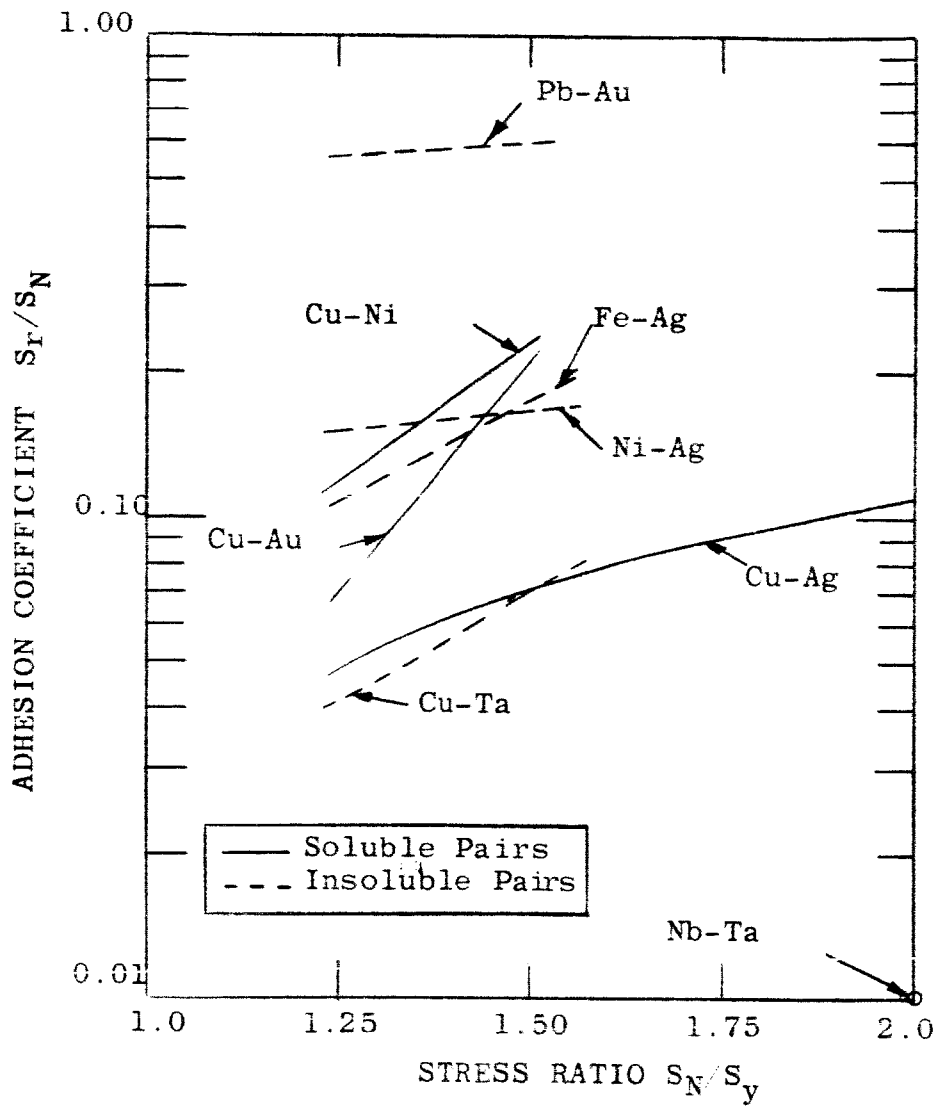


Fig. 12 Variation of the adhesion coefficient with yield coefficient for soluble and insoluble metal pairs.

The product of the adhesion coefficient and yield coefficient provides a measure of the bond efficiency:

$$(S_r/S_N) (S_N/S_y) = S_r/S_y \quad (1)$$

For complete surface welding, $S_r = S_y$ and the bond efficiency would be unity. In Table III, the maximum bond efficiency for each sample pair is tabulated. It is apparent that most of the sample pairs tested fall in the range 0.1 - 0.3 indicating that only about 10 - 30% of the bearing area is in atomic contact. In the case of lead-gold, however, the efficiency rose to 0.9 indicating almost complete bonding.

The adhesion dependency on the yield strength or ductility is illustrated in Fig. 13 in which the variation of the bond efficiency S_r/S_y with yield strength S_y is plotted. For the unlike metal pairs, the lower yield stress was selected as the appropriate value. Although considerable scatter in the experimental values was observed, it was apparent that the adhesion strength generally decreased as the yield stress increased.

Variations in the bond strength at any stress level may be attributed to differences in surface cleanliness since the metallic oxides differ widely in the ease with which they can be abraded off the contact surfaces in vacuum.

In addition to the room temperature tests, measurements of the adhesion properties at 150°C were also obtained. The results given in Fig. 14 show the general increase in adhesion coefficient with temperature for a constant yield coefficient of 1.50. It is evident that the insoluble metal pairs tested exhibited less temperature dependency in general than soluble pairs.

It may be noted that in the case of the insoluble lead-gold pair, the resultant bond strength was greater than the yield stress for lead at 115°C and fracture occurred in the lead sample. This behavior is reflected

TABLE III

Bond Efficiency of Adhesion Samples

<u>Sample Pairs</u>	<u>Yield Coefficient</u> (S_N/S_y)	<u>Adhesion Coefficient</u> (S_r/S_N)	<u>Bond Efficiency</u> (S_r/S_y)
<u>Soluble Pairs</u>			
Cu-Ni	1.25	0.12	0.15
Cu-Ni	1.50	0.23	0.34
Cu-Au	1.25	0.07	0.09
Cu-Au	1.50	0.21	0.32
Au-Ag	1.25	0.05	0.06
Au-Ag	1.50	0.07	0.11
Au-Ag	2.00	0.11	0.22
Nb-Ta	2.00	0.01	0.02
<u>Insoluble Pairs</u>			
Cu-Ta	1.25	0.04	0.05
Cu-Ta	1.50	0.07	0.11
Ag-Fe	1.25	0.11	0.14
Ag-Fe	1.50	0.18	0.27
Ag-Ni	1.25	0.15	0.19
Ag-Ni	1.50	0.17	0.25
Pb-Au	1.25	0.56	0.70
Pb-Au	1.50	0.60	0.90

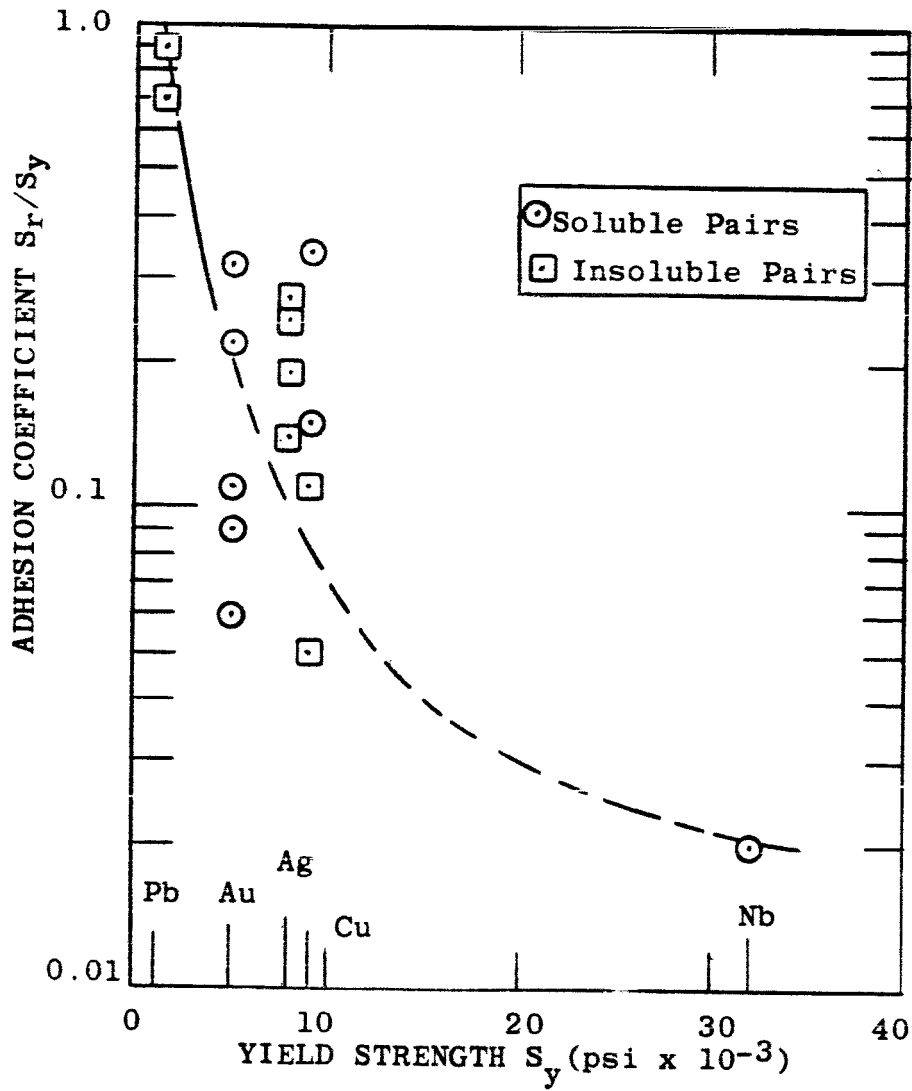


Fig. 13 Adhesion coefficient dependence on the yield strength.

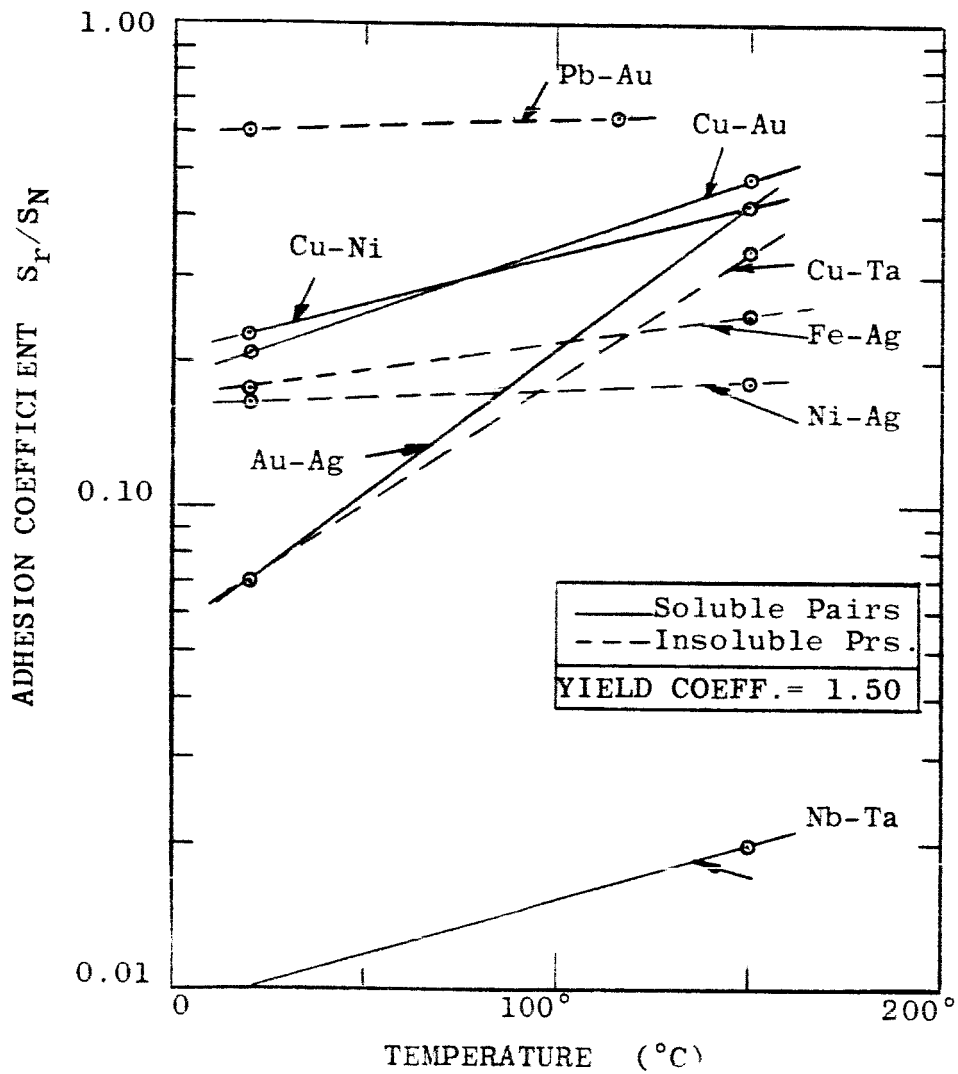


Fig. 14 Temperature dependence of the adhesion coefficient.

in the adhesion coefficient value of 0.66. The efficiency of bonding S_R/S_Y for this sample pair was $1.5 (0.66) \approx 1.0$. In the other tests, fracture always occurred at the interface indicating fractional bond efficiencies.

DISCUSSION

An aspect of the adhesion experiments of great importance is the question of the effectiveness of the ion bombardment technique in removing surface contaminant films prior to contact. Calibration experiments on target areas of copper and tungsten showed that substantial changes in electron work function values were produced by bombardment indicating that the surface atom configuration was being changed. However, subsequent adhesion tests with copper and silver samples using the standard 0.140 sq. in. contact surface area showed that negligible self-adhesion occurred after bombardment.

The low adhesion results may be attributed to several factors which may have operated concurrently. An important parameter is the ion current density and energy maintained during bombardment. It has been established that the inert gas ions will penetrate into the metal lattice if they impact with energies exceeding several hundred volts. Apparently, energetic argon or xenon ions form substitutional solid solutions with the target metal and subsequently diffuse to the surface as shown by annealing experiments in vacuum. Since the energy levels used in the present work here in the range 3,000 - 6,000 volts, it may be inferred that trapped gas ions acted to prevent extensive bare metal contact.

On the basis of these results, it may be suggested that the ion bombardment technique be revised to greatly increase the total impingement energy by increasing the ion current level to the 10^{-3} amp range and to flash heat the samples after bombardment to permit trapped gas ions to diffuse out of the surface. To effectively remove tenacious surface oxides, the bombardment energies must induce surface sputtering over large areas, removing metal substrate layers as well as surface impurity films.

Although a complete analysis of the effect of surface contour on adhesion strength was not attempted, the experimental data showed that surface finish is an important parameter in engineering aspects of solid state bonding. To achieve macroscopic levels of bonding, it is necessary to maximize the extent of metal contact across the interface. Hence, polished surfaces would be expected to show a greater degree of bond strength than roughened surfaces in which a small fraction of the nominal bearing area is in actual contact.

Although plastic deformation at the tips of asperities in contact may be expected, weldments at localized asperity junctions under relatively light loads may not be detected in the apparatus used in this investigation. The minimum detectable bonding force in this apparatus was 10 lbs. Assuming that the stress in the welded asperities at separation was comparable to the gross yield stress, then the minimum detectable area of contact is:

$$A \text{ (min)} = 10/S_y \quad (2)$$

Taking $S_y = 9000$ psi in the case of annealed copper, then the required contact area would be about 10^{-3} sq. in.

Since the total bearing area in the samples is 0.14 sq. in., at least 0.7% of the surface must be in atomic contact for any bonding to be detected. Although it is difficult to estimate the actual contact area, estimates of the asperity areas in contact are usually about $10^{-2}\%$ of the nominal surface for most engineering materials. Hence, determinations of the extent of asperity welding will generally require an extremely sensitive load measuring apparatus.

It may be surmized that although sharp asperities (high height to width ratios) will bond even under light loads due to the high stress operating at the local interface, enlargement of the contact area by plastic flow will rapidly require greatly increased bearing loads as the asperities are blunted. For large scale bonding, it is

apparent that metallic ductility or ease of plastic flow will rapidly dominate the adhesion behavior. Metals of limited ductility will be limited to bonding at microscopic asperities and welding on an engineering scale will not be observed. Asperities in ductile metals, on the other hand, will easily be blunted under deforming loads until relatively smooth surface configurations are assumed.

The dominating importance of plasticity in determining the extent of adhesion at room temperature is emphasized in comparing the bonding behavior of soluble and insoluble metals. Ductile metals were observed to readily adhere although possessing extremely limited bulk solid solubility.

The relative insensitivity of bonding to interatomic accommodation in the bulk lattice may be attributed to the importance of the local atom distribution in the surface layers in controlling adhesion. Increases in the effective lattice parameter and local disorder at the surface may be expected due to the anisotropy of atomic packing and bond distribution. In this way, solute atoms of greatly differing size and electrochemical activity may be accepted substantially or interstitially in the solvent lattice within a few atomic layers of the surface, but would be rejected in the bulk lattice.

In bonding chemically insoluble metals, thermal diffusion across the interface would be expected to produce intermetallic compound or terminal phase precipitation and segregation. The experimental results at 150°C show that brittle compound formation at this temperature was negligible for the materials tested since separation occurred at the original interface. The increase in adhesion noted with the higher temperature may be related to the lowering of the yield stress or increase in ductility usually found for most metals.

CONCLUSIONS

A variety of adhesion experiments have emphasized the dual importance of surface cleanliness and ductility in governing the extent of interfacial contact and bonding.

Attempts to remove surface oxides over large contact areas by argon or xenon ion bombardment were only partially successful in the case of copper. Metals possessing strongly adherent oxide films such as silver apparently require more energetic methods for large scale film removal.

The presence of contaminant films and the plastic flow of the surface under load are two most important parameters controlling the extent of bare metal contact across the interface. The lower adhesion values obtained for rough surfaces compared to smooth polished surfaces may be understood as arising from the difference in the amount of atomic interfacial contact with type of surface contour. For extremely plastic metals, the original surface profile will probably have little effect on the extent of metallic contact under deforming loads.

Comparative measurements of the bonding characteristics of soluble and insoluble metals indicated that bulk chemical solubility concepts are of relatively little importance in diffusion-less adhesion limited to the outer surface layers. For practical welding over large surfaces, the extent of bare metal contact in determining the bond efficiency is probably of greater importance than the intrinsic unit bond strength between various metal atoms.

FUTURE WORK

The research effort on metallic adhesion at National Research Corporation has concentrated up to the present on the surface sensitive parameters controlling bonding such as cleanliness, yield strength and ductility and solid solubility concepts.

In future work, the experimental effort will be extended to considerations of the effect of lattice structure, bond coordination number and lattice orientation on the extent of adhesion. For this purpose, comparative adhesion tests of metals with similar mechanical properties will be made as a function of lattice structure and phase transformations. Experiments will also be conducted on single crystals to determine the influence of lattice orientation on the degree of bonding.